Supplementary Material

Effectiveness of a novel gene nanotherapy based on putrescine for cancer treatment

Saínza Lores[1,2], Manuel Gámez-Chiachio[3,4], María Cascallar[1,2,4], Carmen Ramos-Nebot[3,4], Pablo Hurtado[2,5], Sandra Alijas[5], Rafael López López[1,2,4,5], Roberto Piñeiro[4,5], Gema Moreno-Bueno[3,4,6*], and María de la Fuente[1,4,7*]

[1] Nano-Oncology and Translational Therapeutics Unit, Health Research Institute of Santiago de Compostela (IDIS), Travesía da Choupana s/n, Santiago de Compostela, 15706, A Coruña, Spain; sainza.lores@gmail.com; maria.cascallarc@gmail.com

[2] Universidade de Santiago de Compostela (USC), Praza do Obradoiro, s/n, Santiago de Compostela, 15782, A Coruña, Spain.

[3] Translational Cancer Research Laboratory, Department of Biochemistry, Autonomous University of Madrid, School of Medicine, "Alberto Sols" Biomedical Research Institute CSIC-UAM, IdiPaz, Arturo Duperier 4, 28029, Madrid, Spain; mgamez@iib.uam.es; Carmen Ramos cramos@iib.uam.es

[4] Cancer Research (CIBERONC), 28029 Madrid, Spain

[5] Roche-CHUS Join Unit. Translational Medical Oncology Group (ONCOMET); Health Research Institute of Santiago de Compostela (IDIS), Travesía da Choupana s/n, Santiago de Compostela, 15706, A Coruña, Spain; felurh@gmail.com; sandraalijasperez@gmail.com; rafa.lopez.lopez@gmail.com; Roberto.Pineiro.Cid@sergas.es

[6] MD Anderson Foundation, 28033 Madrid, Spain

[7] DIVERSA Technologies SL, Edificio Emprendia, Campus Vida s/n, Universidade de Santiago de Compostela, 15782 Santiago de Compostela, Spain

***** Correspondence: maria.fuente.freire@sergas.es, gmoreno@iib.uam.es; Tel.: +34 981-955-706

Keywords: Putrescine; Non-viral vector; Putrescine sphingomyelin Nanosystems; Cancer; Gene Therapy; Zebrafish.

Supplementary Material

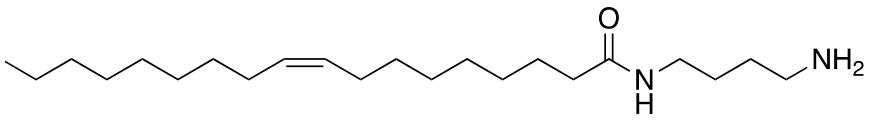

Figure S1. Chemical structure of the putrescine-lipid derivative

a)

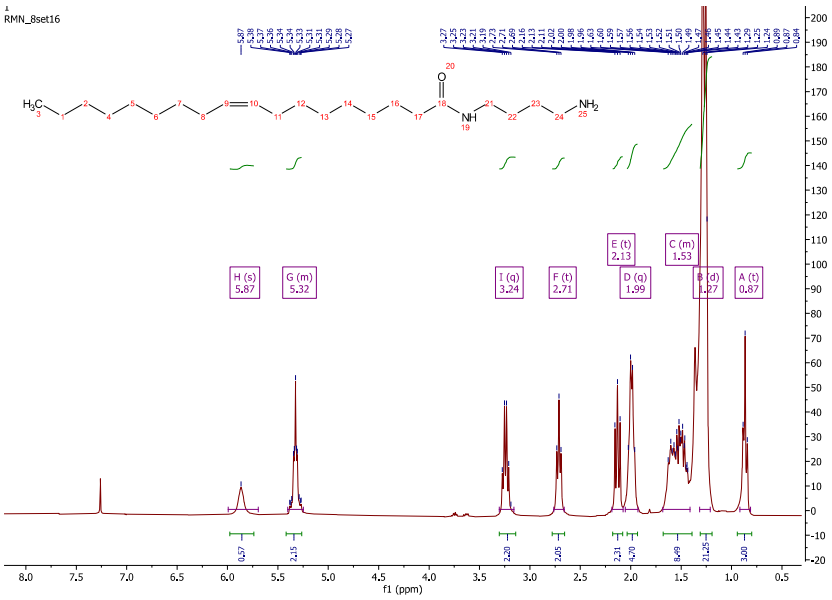

b)

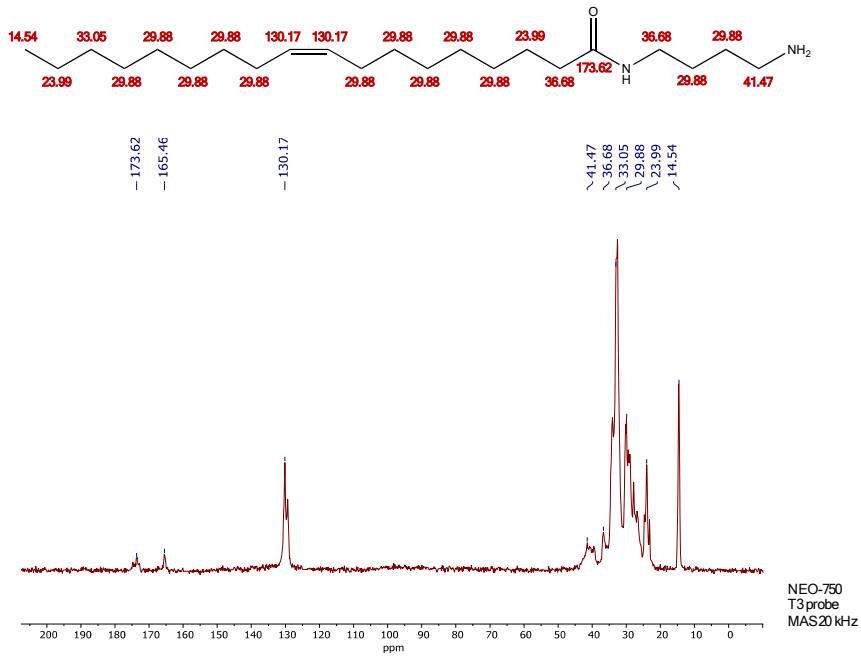

Supplementary Material

c)

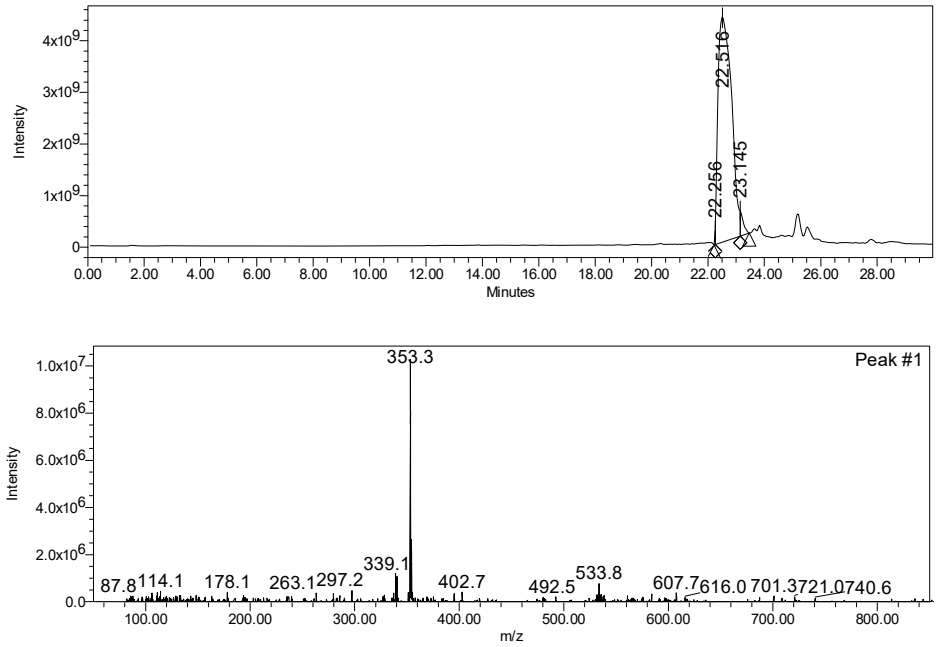

Figure S2. Analytical evaluation of the putrescine-lipid derivative by a) ^{1}H-NMR, b) ^{13}C-NMR, and c) HPLC-MS/UPLC-MS

Table S1. Physicochemical characterization of nanosystems with 5mg of Vitamin E and sphingomyelin (SM) or lipid-derivative putrescine (C18-Pt), or non-modified putrescine (Pt). Mean ± SD (n≥3).

#	SM (µg)	C18-Pt (µg)	Pt (µg)	Size (nm)	PdI[a]	ZP[b] (mV)
G	500	0	0	111 ± 4	0.11	- 31 ± 5
H		50		113 ± 5	0.20	+ 55 ± 1
I	0	250	0	103 ± 10	0.20	+ 62 ± 5
J		500		111 ± 8	0.22	+ 62 ± 6
K	0	0	250	1078 ± 588	0.34	+ 43± 16

[a] PdI: Polydispersity Index; [b] ZP: Zeta Potential

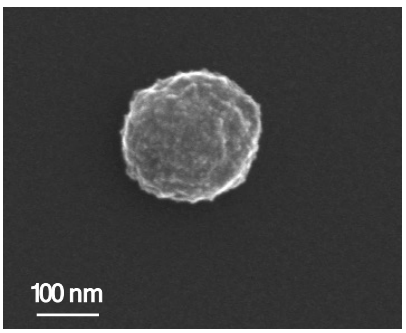

Figure S3. PSN-pDNA evaluated by Scanning Transmission Electronic Microscopy with an InLens detector.

Supplementary Material

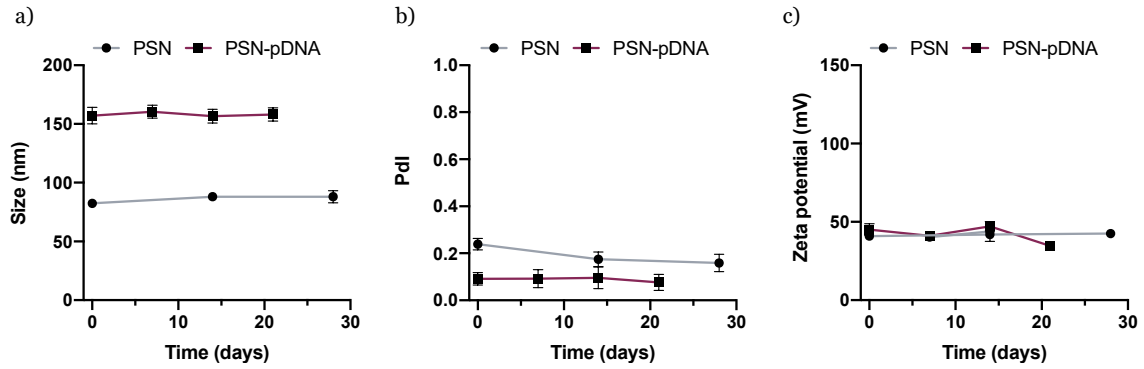

Figure S4. Stability evaluation of PSN and PSN-pDNA under storage conditions (4°C) in terms of a) size, b) PdI, and c) Zeta potential.

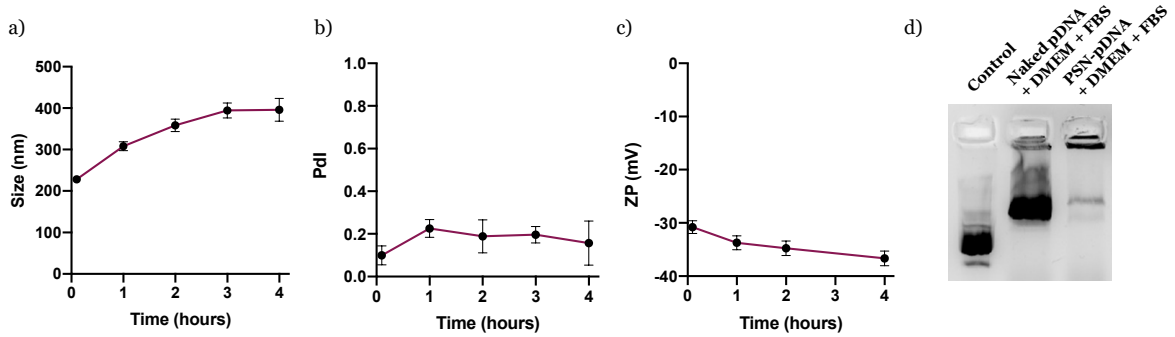

Figure S5. Physicochemical characterization of PSN-pDNA upon incubation with supplemented DMEM in terms of a) size, b) PdI, c) Zeta potential, and d) pDNA displacement

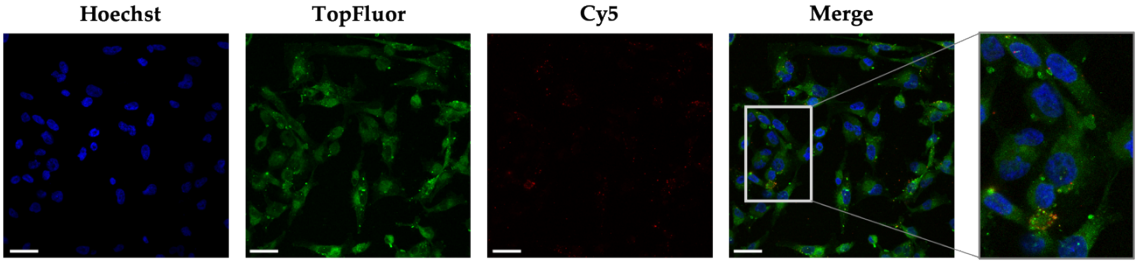

Figure S6. Confocal images of PSN-pDNA after 4 h of incubation in MDA-MB-231 cells. TopFluor-labelled PSN (green), Cy5-pDNA (red), nuclei (blue). Scale bars, 25 μm.

Supplementary Material

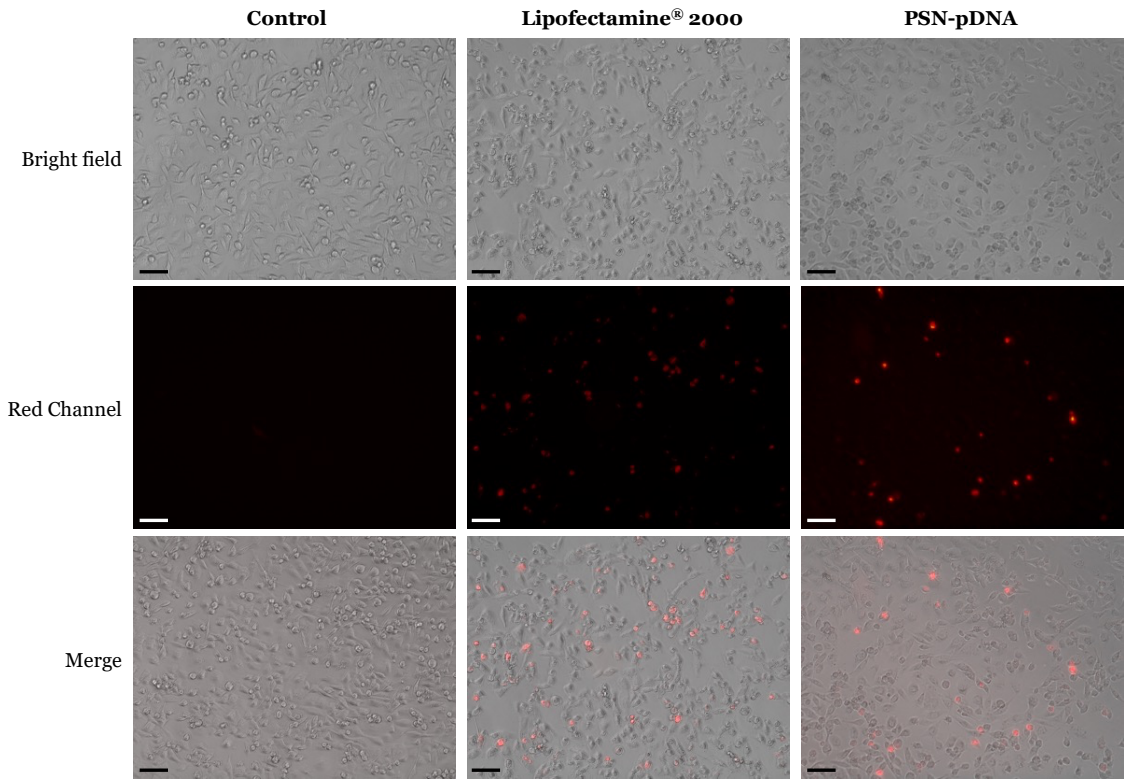

Figure S7. mCherry signal observed under the fluorescence microscope after 24h post-transfection of MDA-MB-231 cells. Scale bars, 50 μm.

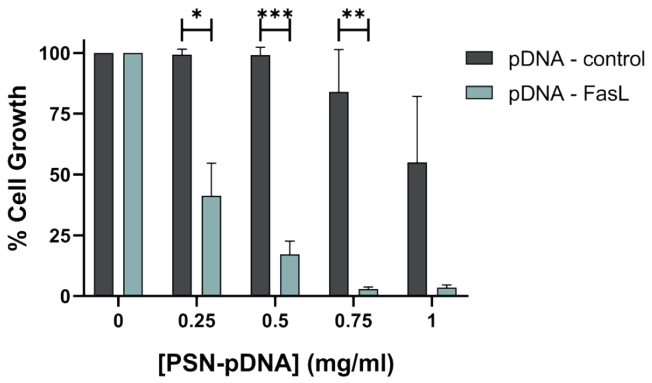

Figure S8. Cytotoxic effect of PSN-pDNA-FasL treatment in HCC38 cells was evaluated with different concentrations by cell viability assay. Statistical significance was determined by two-tailed unpaired t-test (*$p < 0.05$; **$p < 0.01$, ***$p < 0.001$). Data are shown as the mean ± SEM. Three independent experiments were performed.

Supplementary Material

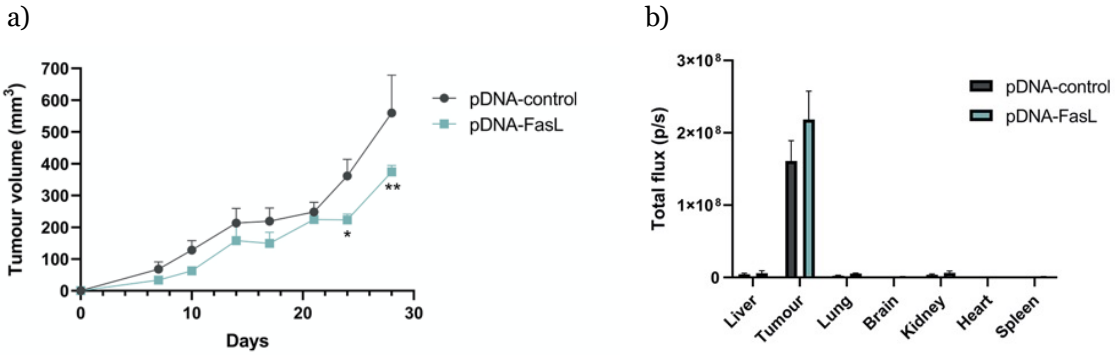

Figure S9. Cytotoxic effect of PSN-pDNA-FasL treatment in mice. (a) Quantification of tumour volume evolution of MDA-MB-231 mouse xenografts, treated with the indicated regimens via intratumoral (n=3 per condition). Statistical significance was determined by multiple unpaired t-test – comparing both treatments at every time point. (b) Biodistribution of TopFluor-labelled pDNA-control or pDNA-FasL treated via intratumoral. Quantification of the TopFluor fluorescence of the indicated organs *ex vivo* was performed by normalizing it to the organs' background from untreated mice. Bars represent mean ± SEM. *p <0.05; **p<0.01; ***p < 0.001; ****p < 0.0001

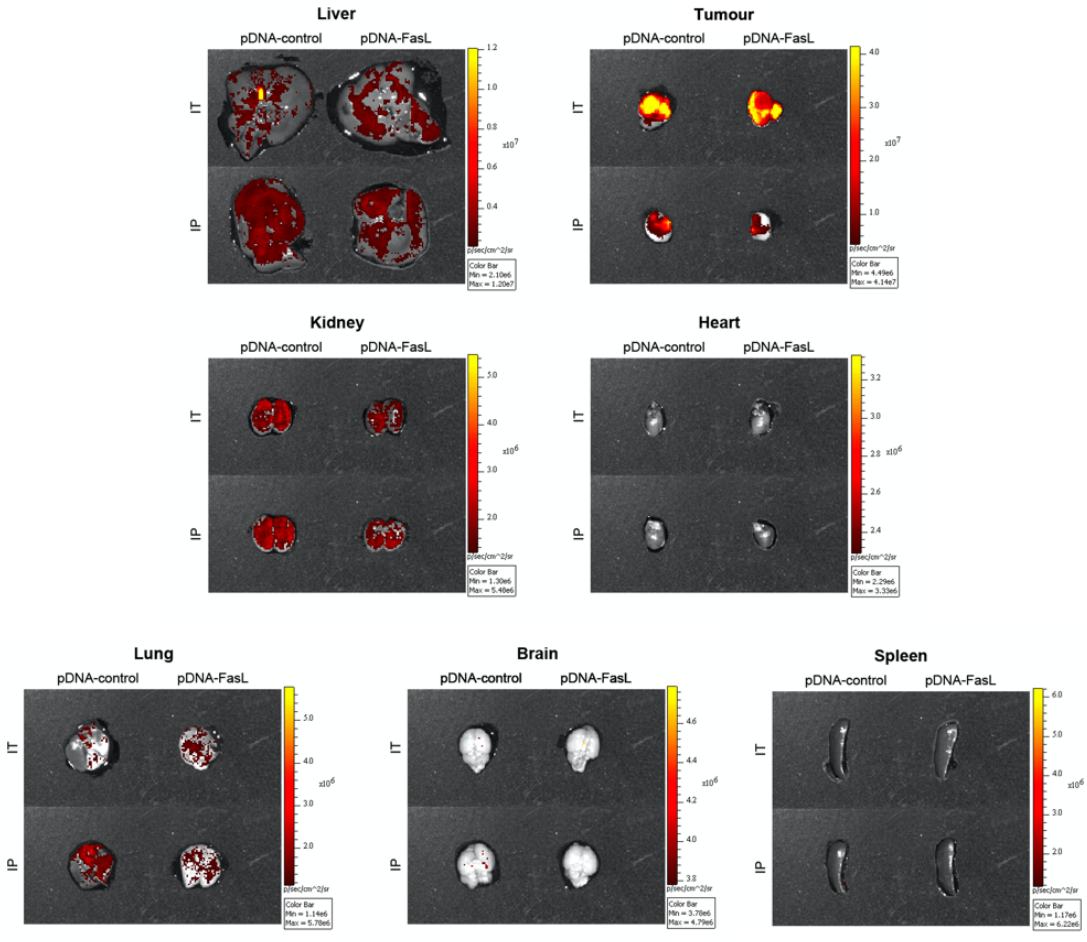

Figure S10. pDNA-control and pDNA-FasL efficiently target breast tumours *in vivo*. Representative images of the *ex vivo* TopFluor fluorescent signal of the different organs of each indicated treatment. IT, intratumoral. IP, intraperitoneal.